Biodiversity buffers the response of spring leaf unfolding to climate warming

Chaoyang Wu (wucy@igsnrr.ac.cn)
Institute of Geographic Sciences and Natural Resources Research https://orcid.org/0000-0001-6163-8209

Pengju Shen
Institute of Geographic Sciences and Natural Resources Research

Xiaoyue Wang
The Key Laboratory of Land Surface Pattern and Simulation, Institute of Geographical Sciences and Natural Resources Research, Chinese Academy of Sciences

Constantin Zohner
ETH Zurich https://orcid.org/0000-0002-8302-4854

Josep Penuelas
CSIC, Global Ecology Unit CREAF-CSIC-UAB, Cerdanyola del Vallès 08193, Catalonia, Spain
https://orcid.org/0000-0002-7215-0150

Yuyu Zhou
The University of Hong Kong https://orcid.org/0000-0003-1765-6789

Zhiyao Tang
Peking University

Jianyang Xia
East China Normal University https://orcid.org/0000-0001-5923-6665

Hua Zheng
State Key Laboratory of Urban and Regional Ecology, Research Center for Eco-Environmental Sciences, Chinese Academy of Sciences

Yongshuo Fu
Beijing Normal University

Jingjing Liang
Purdue University

Weiwei Sun
Ningbo University

Yongguang Zhang
Nanjing University https://orcid.org/0000-0001-8286-300X

Article

Keywords:

Posted Date: November 28th, 2023

DOI: https://doi.org/10.21203/rs.3.rs-3429918/v1

Additional Declarations: There is **NO** Competing Interest.

Abstract

Understanding the sensitivity of spring leaf-out dates to temperature (S_T) is integral to predicting phenological responses to climate warming and the consequences for global biogeochemical cycles. While variation in S_T has been shown to be influenced by local climate adaptations, the impact of biodiversity on phenological sensitivity remains unknown despite its central role in ecosystem functioning. Here, we combine 393,139 forest inventory plots with satellite-derived S_T across the Northern Hemisphere during 2001-2021 to show that biodiversity greatly affects spatial variation in S_T and even surpasses the importance of climate variables. High tree diversity significantly weakened S_T, possibly driven by both more diverse responses of leaf unfolding timing to warming directly, and indirect changes associated with root depth and soil biogeophysical and biogeochemical processes. We further show that current Earth System Models failed to reproduce the observed negative correlation between S_T and biodiversity, with important implications for phenological responses under future emission pathways. Our results highlight the need to incorporate the buffering effects of biodiversity to better understand the impact of climate warming on spring leaf unfolding and carbon uptake in terrestrial ecosystems.

Introduction

Plant phenology is one of the most sensitive indicators of climate change, and greatly affects interannual variations in carbon uptake of terrestrial ecosystems[1,2]. Over recent decades, climate warming has led to strong advances in spring leaf-out dates[3,4]. The responsiveness of spring phenology to climate change is typically quantified via measuring the temperature sensitivity of leaf-out (S_T, leaf-out advance in days per each degree air temperature warming). Understanding temporal and spatial variation in S_T is critical to better comprehend phenological feedbacks to climate change, such as effects on carbon sequestration[5], surface albedo and the energy budget[5,6]. Declines in S_T have been observed in several tree species over recent decades. Yet, although decreased winter chilling has been suggested as a possible factor, the underlying causes remain poorly understood[7]. While previous studies have mostly focused on the climatic drivers of S_T, we still lack an understanding of the responses of S_T to changes in the biodiversity of animals, plants, and microorganisms and the communities they form[8].

Biodiversity plays a crucial role in regulating the growth and development of vegetation, serving as a key factor in stabilizing and adapting ecosystems to climate change[9]. Several studies have indicated that warming-induced changes in spring leaf-out may lead to asynchronous interactions among associated species within communities, affecting food web dynamics and the functioning and stability of ecosystems[2,3,10,11]. In particular, high biodiversity can influence the phenological plasticity of individual plants, enhance the adaptability of plants to climatic shifts, diminish the likelihood of phenological discordance, and affect the species assemblage and functional heterogeneity of plant communities, thereby mitigating the effects of climate change on ecosystem performance[12,13]. For example, different genotypes or genera of plants can adapt to variations in temperature and moisture by altering gene

expression, hormone levels, leaf area, and other parameters that affect phenology[14]. Different species have different phenological strategies to cope with environmental fluctuations, and higher temporal complementarity and asynchrony among species can augment their resistance to drought[15]. Regions with high biodiversity thus typically have stabler ecosystem responses to climate change, whereas the loss of diversity may aggravate plant phenological shifts caused by climate change[9,11,12]. In this study, we therefore aimed to test whether biodiversity buffers the sensitivity of trees to climate warming and how interactions between biodiversity and climate change affect Northern Hemisphere-wide phenological variation.

Results

We compiled tree diversity data from more than 393,139 forests inventory plots from the Global Forest Biodiversity Initiative (GFBI), encompassing a wide range of forest types and species (Supplementary Fig. 1). Satellite-derived leaf-out data from 2001–2021 came from the Moderate-resolution Imaging Spectroradiometer (MODIS). We also gathered spatially-explicit climate and soil data from 2001–2021, as well as gross primary production (GPP) data from 15 Trendy models for 2001–2021 and 13 Cmip6 models for 2016–2100 (Supplementary Table 1–3). For each forest plot, we calculated the optimal spring pre-season period using partial correlation analysis and calculated S_T using ordinary least squares regression. We then used partial correlation, structural equation modeling, and machine-learning methods to determine the influence of biodiversity on S_T and its underlying mechanisms at regional and global levels (see Methods).

The partial correlation analysis showed a predominantly negative correlation between biodiversity and S_T at the local scale after removing the effects of spring and annual temperature, radiation, precipitation, soil moisture, soil organic C (SOC), soil nitrogen (N) and forest age (Fig. 1A), with 61.6% of the correlations being negative. Twelve percent of the local correlations were significantly negative ($P < 0.05$), while significant positive correlations were only found for 4.7% of the correlations. The partial correlation analysis showed consistent results at the levels of plant functional types (Fig. 1E, F), forest biomes (Fig. 1G, H), and Köppen-Geiger climatic zones (Fig. 1I, J). For example, negative correlations were found among eight of eleven plant functional types, with six being significant, while the correlations in Evergreen Broadleaf Forests (EBF) and Deciduous Broadleaf Forests (DBF) were not significant. Similarly, five of the eight biomes showed a negative correlation, and all five correlations were significant, with only deserts and xeric shrublands (DXS), Tundra (TUN), Tropical and Subtropical Grasslands (TSG) showing a non-significant positive correlation. Furthermore, Biodiversity and S_T were negatively correlated in 9 of 11 climatic zones (eight were significant) and positively correlated in the other two zones (DFA (Cold, no dry season, hot summer) and DSB (Cold, dry summer, warm summer)).

In a next step, we analyzed the relative importance of biodiversity in determining the changes in S_T using machine learning (Random Forest and eXtreme Gradient Boosting (XGBoost) models). We found that biodiversity was a more important driver of S_T than were temperature, precipitation, solar radiation, and

soil moisture, SOC, and N (Fig. 1C, D and Extended Data Fig. 1). Additionally, the SHapley Additive exPlanations (SHAP) values of Random Forest and XGBoost models also showed a predominantly negative effect of biodiversity on S_T, confirming the linear partial correlation analyses. The feature importance (GINI and SHAP importance, Fig. 1C) and absolute coefficients of the partial correlation all supported biodiversity as the most important driver of S_T (Fig. 1B).

To test the possible mechanisms through which biodiversity may affect S_T, we applied Structural equation modeling (SEM) and partial correlation analysis (Fig. 2). We calculated the direct effects of biodiversity on S_T within the SEM and the indirect effects through different pathways. The results indicate a strong direct effect of biodiversity. In addition, root depth, soil organic carbon concentration, the soil carbon-to-nitrogen (C/N) ratio, and soil physical properties (including bulk density and volumetric fraction of coarse fragments (VOCF)) may be potential intermediaries between biodiversity and phenological responsiveness. For example, biodiversity and the C/N ratio were mostly positively correlated, with 20.2% and 7.4% of correlations being significantly positive and negative, respectively. The correlation between the C/N ratio and root depth was also positive, with 30.0% of the correlations significantly positive and only 7.0% of the correlations significantly negative. In comparison, root depth and S_T were generally negatively correlated. Similarly, a higher SOC concentration was associated with increased biodiversity, but SOC concentration and S_T were negatively correlated. Soil physical properties may also contribute to the negative relationship between biodiversity and S_T. Biodiversity and bulk density, bulk density and the rate of soil warming in spring (RSWS), and RSWS and S_T were each consistently negatively correlated, with the percentages of significant positive / negative correlations being 10.9% / 31.0%, 18.5% / 53.9%, and 16.0% / 37.7%, respectively. In contrast to bulk density, a higher VOCF was associated with increased biodiversity, and biodiversity increased as S_T decreased, because VOCF and S_T were negatively correlated. Overall, both the direct and the indirect pathways support the negative correlation between biodiversity and S_T.

We further tested whether state-of-the-art ecosystem models (15 Trendy models with results over 2001–2021 and 13 Cmip6 models over 2016–2100) can reproduce the negative correlation between S_T and biodiversity (Fig. 3). We found that most Trendy models do not capture the observed relationships, with 10 out of 15 models simulating predominantly positive correlations (positive correlations exceeding 60%) and only two of the models reproducing the extent of observed negative correlations (negative correlations exceeding 60%, ISAM and ORCHIDEE models). The spatial variation in the correlations simulated by the Trendy models is shown in Fig. 3A1-A15. The Cmip6 models also failed to represent the negative correlation between S_T and biodiversity (Fig. 3B-D). We found that only 2 (out of 13) models (CMCC-CM2-SR5, CMCC-ESM2) had negative S_T-biodiversity relationship exceeding 60% under ssp126. The number of correct models increased to 6 for ssp245 and ssp585, respectively. Spatial distributions of Cmip6 models were provided in Supplementary Fig. 2–4. We also tested for spatial consistency between the observations and simulations and found that most models did not match the observed biodiversity effects closely (Extended Data Fig. 2).

Discussion

Our findings demonstrate a widespread buffering effect of biodiversity on the sensitivity of spring leaf-out dates to climate warming, with weaker responses of spring leaf-out to warming in forests with multiple species. Our models further showed that biodiversity was more important than climate in driving spatial variation in S_T (Fig. 1B-D and Extended Data Fig. 1), highlighting the importance of considering biodiversity when predicting the consequences of climate change on spring phenology and ecosystem productivity. We further showed that current ecosystem models could not reproduce the observed buffering effect of biodiversity on spring phenological sensitivity. Accounting for spatial and temporal variation in species richness will thus be of great importance to better understand the extent of shifts in foliar phenology under climate change as well as the consequences for ecosystem functioning.

We found that biodiversity has a strong direct impact on S_T in our study. We observed that in forests with higher biodiversity, the sensitivity of tree leaf unfolding to climate warming is lower. This suggests that in ecosystems with greater biodiversity, the timing of spring leaf unfolding remains more stable in the face of warming, consistent with recent research[11,12,16]. This direct effect can be partly attributed to the presence of a greater variety of species and individuals in biodiverse forests, where different tree species may have distinct growth seasons and leaf unfolding times. This seasonal asynchrony may, to some extent, slow down the overall response of the ecosystem to rising temperatures[17,18]. Consequently, the entire ecosystem exhibits lower average temperature sensitivity. Conversely, in forests with relatively lower biodiversity, often dominated by a few key species, the response is more uniform, and leaf unfolding is more directly influenced by temperature increase.

While our analyses suggest a strong direct impact of biodiversity on S_T, they also suggest that biogeophysical and biogeochemical factors may contribute to the decrease in S_T with increasing biodiversity. We found that high biodiversity correlates with deeper roots, which may facilitate access to soil nutrients and moisture during spring[19] (Extended Data Fig. 3). The enhanced water supply may in turn reduce trees' sensitivity to temperature early in the growing season, buffering against warming-induced shifts in foliar phenology[9] (Extended Data Fig. 4). In agreement with this, experiments and observations have shown reduced leaf-out sensitivity to warming under drought conditions[1,7]. Our results also agree with studies reporting an increased importance of soil moisture in determining the distribution of vegetation and SOC in cold regions where warming is more pronounced[20].

Our findings also support that higher biodiversity enhances the SOC concentrations in diverse forests by fixing more C[9,13,21]. This may be due to improved soil physicochemical properties, such as VOCF and pH (Extended Data Fig. 5), which in turn accelerate the activities of both plants and soil microorganisms[8,21,22]. Enhanced soil fertility is advantageous for plants because it promotes plant growth and enables roots to anchor more deeply, facilitating more effective adaptation to temperature changes[9]. Increasing soil fertility can in turn increase the diversity of plants and soil microbes, increasing the stability and resilience of ecosystems. We also found that higher biodiversity increased the C/N ratio,

which may limit the availability of N for plants and cause them to allocate more C to root growth to enhance the uptake of water and nutrients while reducing foliar growth to save energy for photosynthesis and transpiration[23].

Higher biodiversity also improved soil biogeophysical properties, providing better soil aeration, thermal conductivity, and water retention. These improvements may be associated with increased soil microbial activity and plant root growth[19,22]. The improvement of soil physical properties, especially water retention and buffering capacity, has been demonstrated to enhance the resistance of plants to stress, thus alleviating the response of plants to warming and consequently improving phenological stability[19,21]. Our results also showed that S_T becomes less dependent on warming for wetter conditions induced by higher biodiversity (Extended Data Fig. 4B). Better soil aeration and thermal conductivity can increase RSWS and its variability, causing a higher frost risk. To avoid such risks, plants may therefore increasingly rely on other signals, such as photoperiod and higher chilling requirements, leading to declines in S_T[24,25]. Enhancement of soil physical properties affects the growth of plant roots and the retention of SOC and N[19,21] (Fig. 2), and increased rooting depth and supply with soil nutrients is likely to drive phenological stability and reduce S_T.

In summary, our findings show that the sensitivity of spring leaf-out to warming decreases in more diverse forests, suggesting an important buffering effect of biodiversity on the phenological sensitivity of trees to climate change. The biodiversity effects on phenological sensitivity may be of direct and indirect nature. In diverse forests, the high diversity in temperature sensitivity among species and individuals may lead to a lower average temperature sensitivity than in less diverse forest where single species dominate the observed community sensitivity. In addition, the biodiversity effects could be mediated by soil physicochemical properties, which may stabilize phenology by enhancing nutrient supply, stress tolerance, and productivity[12,13,15]. Higher productivity in diverse forests may also lead to changes in ecosystem function due to shifts in species composition and community succession, water balance, and climatic feedbacks[26]. The inability of vegetation models to reproduce the observed buffering effect of tree diversity on phenological sensitivity highlights the need to represent biodiversity if we are to accurately predict ecosystem responses to climate change. Our findings thus underscore the fundamental importance of biodiversity in our understanding of phenological changes and the maintenance of ecosystem functioning under climate change.

Declarations

Data availability

All data used in this study are available online. The specific links for each dataset are presented in Supplementary Table 1-3.

Code availability

All data analyses and modeling were performed using Python and R. The codes for the phenological models are available at https://doi.org/10.5281/zenodo.5829780. Other codes are available upon request to the corresponding authors.

Acknowledgements

This work was funded by the National Natural Science Foundation of China (42125101). J.P. was funded by the TED2021-132627B-I00 grant funded by the Spanish MCIN, AEI/10.13039/501100011033 and by the European Union NextGenerationEU/PRTR, the Fundación Ramón Areces project CIVP20A6621 and the Catalan government grant SGR221-1333. C.M.Z. was funded by SNF Ambizione grant PZ00P3_193646.

Author contributions

C.W. designed the research. C.W. and P.S. wrote the first draft of the manuscript. P.S. and X.W. performed the data analysis. All authors assessed the research analyses and contributed to the writing of the manuscript.

Competing interests

The authors declare no competing financial interests.

References

1. Gu, H. *et al.* Warming-induced increase in carbon uptake is linked to earlier spring phenology in temperate and boreal forests. *Nat. Commun.* **13**, 3698 (2022).
2. Peñuelas, J., Rutishauser, T. & Filella, I. Phenology Feedbacks on Climate Change. *Science* **324**, 887–888 (2009).
3. Peñuelas, J. & Filella, I. Responses to a Warming World. *Science* **294**, 793–795 (2001).
4. Menzel, A. *et al.* European phenological response to climate change matches the warming pattern. *Glob. Change Biol.* **12**, 1969–1976 (2006).
5. Gao, M. *et al.* Three-dimensional change in temperature sensitivity of northern vegetation phenology. *Glob. Change Biol.* **26**, 5189–5201 (2020).
6. Maina, F. Z., Kumar, S. V. & Gangodagamage, C. Irrigation and warming drive the decreases in surface albedo over High Mountain Asia. *Sci. Rep.* **12**, 16163 (2022).
7. Fu, Y. H. *et al.* Declining global warming effects on the phenology of spring leaf unfolding. *Nature* **526**, 104–107 (2015).
8. Furey, G. N. & Tilman, D. Plant biodiversity and the regeneration of soil fertility. *Proc. Natl. Acad. Sci.* **118**, e2111321118 (2021).
9. Mori, A. S. *et al.* Biodiversity–productivity relationships are key to nature-based climate solutions. *Nat. Clim. Change* **11**, 543–550 (2021).

10. Yin, R. *et al.* Experimental warming causes mismatches in alpine plant-microbe-fauna phenology. *Nat. Commun.* **14**, 2159 (2023).
11. Wolf, A. A., Zavaleta, E. S. & Selmants, P. C. Flowering phenology shifts in response to biodiversity loss. *Proc. Natl. Acad. Sci.* **114**, 3463–3468 (2017).
12. Dronova, I., Taddeo, S. & Harris, K. Plant diversity reduces satellite-observed phenological variability in wetlands at a national scale. *Sci. Adv.* **8**, eabl8214 (2022).
13. Chen, X. *et al.* Tree diversity increases decadal forest soil carbon and nitrogen accrual. *Nature* 1–8 (2023) doi:10.1038/s41586-023-05941-9.
14. Zhang, S., Dai, J. & Ge, Q. Responses of Autumn Phenology to Climate Change and the Correlations of Plant Hormone Regulation. *Sci. Rep.* **10**, 9039 (2020).
15. Liu, D., Wang, T., Peñuelas, J. & Piao, S. Drought resistance enhanced by tree species diversity in global forests. *Nat. Geosci.* **15**, 800–804 (2022).
16. Oliveira, B. F., Moore, F. C. & Dong, X. Biodiversity mediates ecosystem sensitivity to climate variability. *Commun. Biol.* **5**, 1–9 (2022).
17. García-Palacios, P., Gross, N., Gaitán, J. & Maestre, F. T. Climate mediates the biodiversity–ecosystem stability relationship globally. *Proc. Natl. Acad. Sci.* **115**, 8400–8405 (2018).
18. Rheault, G., Lévesque, E. & Proulx, R. Diversity of plant assemblages dampens the variability of the growing season phenology in wetland landscapes. *BMC Ecol. Evol.* **21**, 91 (2021).
19. Gould, I. J., Quinton, J. N., Weigelt, A., De Deyn, G. B. & Bardgett, R. D. Plant diversity and root traits benefit physical properties key to soil function in grasslands. *Ecol. Lett.* **19**, 1140–1149 (2016).
20. Ding, J. *et al.* Decadal soil carbon accumulation across Tibetan permafrost regions. *Nat. Geosci.* **10**, 420–424 (2017).
21. Chen, S. *et al.* Plant diversity enhances productivity and soil carbon storage. *Proc. Natl. Acad. Sci.* **115**, 4027–4032 (2018).
22. Beugnon, R. *et al.* Tree diversity and soil chemical properties drive the linkages between soil microbial community and ecosystem functioning. *ISME Commun.* **1**, 1–11 (2021).
23. Zhang, J. *et al.* Variation and evolution of C:N ratio among different organs enable plants to adapt to N-limited environments. *Glob. Change Biol.* **26**, 2534–2543 (2020).
24. Wang, C., Cao, R., Chen, J., Rao, Y. & Tang, Y. Temperature sensitivity of spring vegetation phenology correlates to within-spring warming speed over the Northern Hemisphere. *Ecol. Indic.* **50**, 62–68 (2015).
25. Wang, T. *et al.* The influence of local spring temperature variance on temperature sensitivity of spring phenology. *Glob. Change Biol.* **20**, 1473–1480 (2014).
26. Shen, M. *et al.* Plant phenology changes and drivers on the Qinghai–Tibetan Plateau. *Nat. Rev. Earth Environ.***3**, 633–651 (2022).

Methods

1. Biodiversity, climate and ancillary data

We focused our research on the Northern Hemisphere (30 °N), where vegetation dynamics exhibit distinct seasonal variations. We extracted biodiversity data covering most of the forests in our study area from the GFBI ground observation dataset[27], which compiles extensive monitoring data from 777,126 permanent plots across 44 countries and 13 ecoregions. The GFBI dataset encompasses diverse forest sources and successional stages, and an excess of 30 million trees belonging to over 8,737 species were measured twice or more, with the aim of unveiling global forest biodiversity patterns.

Due to the large number of duplicate coordinates in the GFBI dataset, we used a window size of 0.01 degrees, the minimum scale of GFBI coordinate records, to extract the maximum value within each window as its corresponding value. In the end, we determined 393,139 distinct biodiversity records, encompassing 1-190 tree species. Notably, deciduous broadleaf forests and woody savannas exhibit the highest species richness per plot scale, averaging 6-7 species per plot, while open shrublands, barren, and grasslands only contain 2-3 tree species (Supplementary Fig. 1).

The leaf-out dates data was determined from Moderate Resolution Imaging Spectroradiometer (MODIS) Land Cover Dynamics (MCD12Q2) dataset, which provides global land surface phenology metrics annually spanning from 2001 to 2021 with a spatial resolution of 500 meters[28]. These metrics are derived from time series data of the two-band Enhanced Vegetation Index (EVI2) computed from MODIS Nadir Bidirectional Reflectance Distribution Function (BRDF)-Adjusted Reflectance (NBAR). One of these metrics, leaf-out dates, is defined as the date when the EVI2 first exceeds 15% of the segment EVI2 amplitude.

The climate data was obtained from monthly data of ERA5-Land dataset, which is the fifth-generation atmospheric reanalysis produced by the European Centre for Medium-Range Weather Forecasts[29]. It has been widely utilized for evaluating the influence of meteorological variables on the Earth's global climate. Specifically, we extracted temperature, total precipitation, solar radiation, and soil moisture data from 2001 to 2021, with a spatial resolution of 0.1 degrees and a temporal resolution of one month from ERA5-Land. Furthermore, we collected hourly soil temperature data and calculated the daily mean for later analysis.

The soil attribute data was derived from SoilGrids, a global soil dataset product resulting from international collaboration generated by the ISRIC - World Soil Information Center, with a resolution of 250 meters[30]. SoilGrids implements advanced machine learning techniques, combining global soil profile data and environmental covariate data to predict and simulate the spatial distribution of soil properties at six standard depths globally. We utilized the latest version of SoilGrids, version 2.0, to extract soil surface organic carbon content, soil total nitrogen content, and subsequently calculated the soil surface carbon-to-nitrogen ratio.

The GPP (Gross Primary Productivity) data was originated from Trendy and Cmip6 model, utilized for the simulation of leaf-out dates across historical and future periods. The Trendy model ensemble

encompassed many models reflecting estimates of terrestrial vegetation photosynthesis and was extensively employed to delve into diverse facets of the global carbon cycle[31]. We curated GPP data spanning from 2001 to 2021, encompassing 15 models (Supplementary Table 2). CMIP6, the Coupled Model Intercomparison Project phase 6, furnishes output data for an array of climate variables under different experimental designs and emission scenarios, encompassing historical and forthcoming epochs[32]. We gathered GPP, temperature, precipitation, radiation, and soil moisture data from 2015 to 2100 across each of 13 models. Each model encompasses three shared socioeconomic pathways: ssp126, ssp245, and ssp585 (Supplementary Table 3).

Auxiliary data includes biomes, vegetation types, climatic regions, and forest age. Biomes data is derived from the Resolve Ecoregions 2017, which serves as a biogeographic regionalization under an Earth's biomes framework, consisting of 14 terrestrial biomes made up of 846 ecoregions, defining biogeographic assemblages and ecological habitats[33] (Supplementary Table 4). Vegetation types data is obtained from the first layer of MCD12Q1 Version 6.1 dataset and represents land cover types in the International Geosphere-Biosphere Programme classification[34]. And thirteen different types of vegetation are present in the study area (Supplementary Table 5). Climatic regions data is procured from the widely utilized Köppen-Geiger climate classification system, which divides the global climate zones into five primary groups based on local vegetation types: tropical, arid, temperate, continental, and polar[35]. Further subdivisions of each group are based on temperature or aridity level (Supplementary Table 6). The forest age data is sourced from the Max Planck Institute for Biogeochemistry in Germany. It provides global forest age estimations at a 1-kilometer resolution, and this data is predicted using machine learning techniques based on forest inventories, biomass measurements, and climate data.

2. Simulating leaf-out dates utilizing GPP data of Trendy and Cmip6 models

We employ GPP data from Cmip6 and Trendy models to simulate leaf-out dates. GPP exhibits a close correlation with factors such as vegetation coverage, Leaf Area Index (LAI), temperature, and precipitation - all pivotal elements influencing vegetative leaf-out dates. Therefore, the annual fluctuation curve of GPP effectively mirrors the phenological cycles of vegetation[36]. Drawing upon this theoretical foundation, we utilized cubic spline interpolation for temporal sequence interpolation to enhance data continuity, considering temporal resolution of most GPP datasets is monthly. Subsequently, we opted for the “phenofit” function package[37] within the R programming language for simulation. To ensure both efficiency and quality in simulating leaf-out dates, we employed the "Elmore" curve fitting method[36]. The fitting function is represented by equation (1) as follows:

$$f(t) = mn + (mx - m_7 t) \times \left(\frac{1}{1+e^{-rsp(t-sos)}} - \frac{1}{1+e^{-rau(t-eos)}} \right) \quad (1)$$

Where *t* is the corresponding date of time series GPP, *mn* and *mx* are the minimum and maximum value of time series GPP; *sos* and *eos*, respectively, denote the start of the growing season and end of the growing season; *rsp* and *rau* are, respectively, the rate of spring Greenup and autumn senescence, m_7 is the summer greendown parameter. Subsequently, based on the fitted curve, we have utilized three different methods to extract leaf-out dates: the threshold method, derivative method, and inflection method. Notably, through meticulous comparisons, the extracted leaf-out dates exhibited harmonious interannual variations across all three methods (Supplementary Fig. 5). To maintain congruity with MCD12Q2, we chose to showcase the 15% threshold method as the primary approach in the main text.

3. Calculating S_T, RSWS

We first aggregated data from multiple sources using the coordinates from biodiversity data. For climate data with coarser resolutions, we directly extracted data from the corresponding locations. For categorical datasets like biomes, we used the mode within the corresponding window size as the representative value, while for continuous datasets like soil properties, we used their mean values within the grid. Subsequently, we standardized all data using the Z-score method to convert metrics of varying units into a uniform scale, and excluded outliers in accordance with the PauTa criterion.

S_T, the sensitivity of leaf-out advance to warming, is defined as the days of advanced leaf-out dates per each degree changes in air temperature. For the purpose of narrative convenience, we shall define the advancement of leaf-out dates as a positive value and the delay as a negative value, which is equivalent to taking the opposite of the temperature coefficient as S_T. It can be calculated using the coefficient of temperature in the regression that relates leaf-out dates to climate variables, as shown in the equation (2):

$$L = \beta_0 + (-\beta_T) \times T + \beta_P \times P + \beta_R \times R + \varepsilon \quad (2)$$

where *L* stands for leaf-out dates, *T*, *P*, and *R* denote the mean spring temperature, precipitation, and radiation, respectively. β_T, β_P, and β_R represent their corresponding regression coefficients, out of which β_T signifies S_T. β_0 is the intercept and ε is the residual term. It is worth mentioning that, for the calculation of mean spring values of climate variables, we employed a partial correlation method to iteratively determine the optimal length of the spring pre-season. For the fitting of the regression equation, we used the OLS (ordinary least squares regression) function provided by the Python “statsmodels” package.

RSWS, the rate of soil warming in spring, is defined as the speed of soil temperature change over a period of 60 days, with 30 days before and 30 days after leaf-out date. To calculate RSWS, we first derived daily soil temperature data from hourly data between 2001 and 2021. Next, we employed the Numpy package in Python to fit the daily mean soil temperature data for the 60-day period in each plot, allowing us to determine the slope (i.e., RSWS) as well as the variance, which represents the degree of temperature variability within each plot.

4. Analysis

We first used partial correlation to investigate the relationship between biodiversity and S_T across all plots. The partial correlation method was implemented using the “pingouin” package in Python. When calculating partial correlation, we controlled for mean annual temperature, precipitation, radiation, soil moisture; mean spring temperature, precipitation, radiation, soil moisture, as well as soil organic carbon and total nitrogen, in order to eliminate the influence of environmental factors.

Furthermore, we utilized the Random Forest and eXtreme Gradient Boosting (XGBoost) machine learning algorithms, along with the SHapley Additive exPlanations (SHAP) method, to measure the impact and importance of biodiversity on S_T. Random Forest and XGBoost are decision tree-based machine learning algorithms that excel in processing large-scale data and high-dimensional features, effectively handling nonlinear relationships between features. Therefore, we implemented the aforementioned methods using “scikit-learn” and “xgboost” packages in python to explore the relationship between S_T, biodiversity, and other environmental variables. The SHAP method, based on game theory, provides a feature importance explanation that enhances our understanding of the contribution and direction of each feature in predicting results within machine learning models. By utilizing the “shap” package in Python, we applied the SHAP method to interpret the trained random forest and XGBoost models. This allowed to obtain the magnitude and direction (positive or negative) of the impact of biodiversity on S_T of each plot (Fig. 1C, D and Extended Data Fig. 1).

In addition, to address possible spatial heterogeneity issues at the global scale, we employed two approaches to conduct analyses at a smaller local scale. Firstly, we divided our study area into different regions, including land cover types, biomes, and climatic regions. We then conducted partial correlation analysis on the data within each region. Besides, we also conducted point-wise analyses. To do this, we first created a distance matrix to group the points into clusters based on their proximity to each other. Then, we used partial correlations to conduct the analysis. To selected the points in each group, we used the golden section method as the search algorithm and the Akaike information criterion (AIC) to determine the optimal bandwidth size.

To investigate the potential mechanisms underlying the impact of biodiversity on S_T, we used two methods at the point level: partial correlation and structural equation modeling (SEM). We hypothesized that the impact of biodiversity on S_T is mediated by its influence on soil physicochemical properties and tree root growth. To test this hypothesis, we developed a structural equation model (SEM) incorporating 6 mediating variables: two soil physical properties (BD and VOCF), two soil nutrient variables (SOC and C/N ratio), RSWS and root depth. Maximum likelihood estimation was used as the target function while Sequential Least Squares Programming (SLSQP) optimization method was employed to estimate the model parameters. Additionally, we calculated various statistics and fit indices to evaluate the applicability and effectiveness of the model, such as GFI (Goodness of Fit Index) and RMSEA (Root Mean Square Error of Approximation). Subsequently, we selected pathways with a GFI exceeding the threshold of 0.9 and p-values less than 0.01 and calculated their mean values. We also used partial correlation

analysis as a supplement to the SEM. With controlling for mean annual temperature, precipitation, and radiation effects, we conducted partial correlation analyses on variables at both ends of each SEM path.

For the data of Trendy and CMIP6 models, we followed the same procedure as described above to calculate S_T and analyze the impact of biodiversity on it. However, due to the coarse resolution and lack of time series in these models, temporal and regional analysis were not possible. To determine the biodiversity effects at each point, we employed the geographically weighted regression (GWR) method. GWR is a spatially local regression model that considers spatial heterogeneity. Throughout the analysis, due to the absence of future biodiversity data and soil attribute data, we assumed they remained constant and resampled them to match the resolution of the models. As for future forest age, we conducted year-by-year accumulation to obtain future forest age. We then conducted GWR to analyze the relationship between the models' S_T and factors including biodiversity, mean annual and mean spring climate variables (temperature, precipitation, radiation), mean annual and mean spring soil moisture, soil organic carbon content, soil nitrogen content and forest age. Simultaneously, we resampled the observed data to the same resolution as each model and calculated the impact of biodiversity on S_T (Supplementary Fig. 6). Finally, we compared the biodiversity effect of the observed results, the Trendy and CMIP6 models, and assessed the accuracy of each model at the pixel scale (Fig. 3, Extended Data Fig. 2, and Supplementary Fig. 2-4).

References

27. Liang, J. *et al.* Positive biodiversity-productivity relationship predominant in global forests. *Science* **354**, aaf8957 (2016).

28. Friedl, M. A., Gray, J. & Sulla-Menashe, D. MODIS/Terra+Aqua Land Cover Dynamics Yearly L3 Global 500m SIN Grid V061 [MCD12Q2]. NASA EOSDIS Land Processes Distributed Active Archive Center. (2022).

29. Muñoz-Sabater, J. ERA5-Land monthly averaged data from 1950 to present. Copernicus Climate Change Service (C3S) Climate Data Store (CDS). (2019).

30. Poggio, L. *et al.* SoilGrids 2.0: producing soil information for the globe with quantified spatial uncertainty. *SOIL* **7**, 217–240 (2021).

31. Yu, Z. *et al.* Forest expansion dominates China's land carbon sink since 1980. *Nat. Commun.* **13**, 5374 (2022).

32. Zhu, B. *et al.* Constrained tropical land temperature-precipitation sensitivity reveals decreasing evapotranspiration and faster vegetation greening in CMIP6 projections. *Npj Clim. Atmospheric Sci.* **6**, 91 (2023).

33. Dinerstein, E. *et al.* An Ecoregion-Based Approach to Protecting Half the Terrestrial Realm. *BioScience* **67**, 534–545 (2017).

34. Friedl, M. A. & Sulla-Menashe, D. MODIS/Terra+Aqua Land Cover Type Yearly L3 Global 500m SIN Grid V061 [MCD12Q1]. NASA EOSDIS Land Processes Distributed Active Archive Center. (2022).

35. Beck, H. E. *et al.* Present and future Köppen-Geiger climate classification maps at 1-km resolution. *Sci. Data* **5**, 180214 (2018).

36. Gonsamo, A., Chen, J. M. & D'Odorico, P. Deriving land surface phenology indicators from CO2 eddy covariance measurements. *Ecol. Indic.* **29**, 203–207 (2013).

37. Kong, D. *et al.phenofit*: An R package for extracting vegetation phenology from time series remote sensing. *Methods Ecol. Evol.***13**, 1508–1527 (2022).

Figures

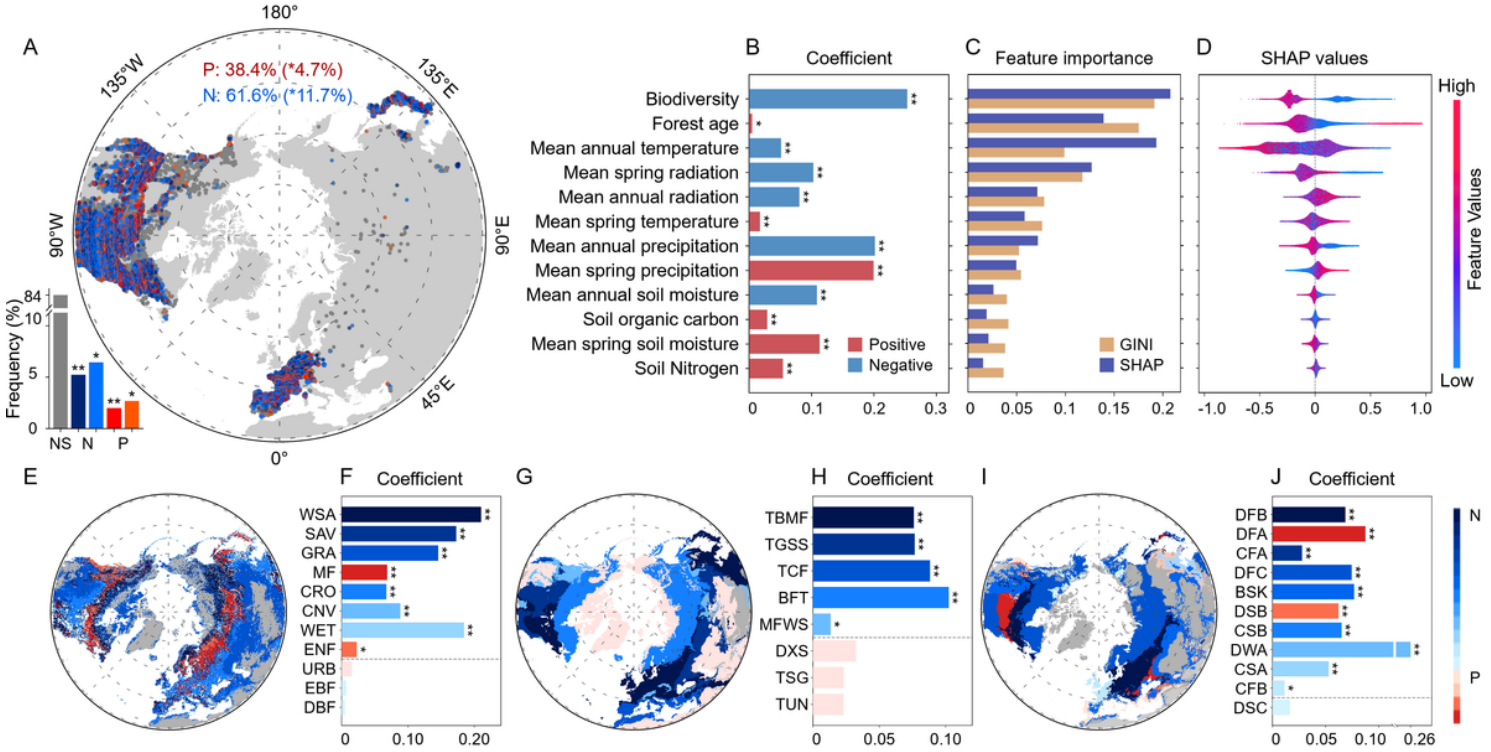

Figure 1

Negative correlations between biodiversity and the sensitivity of spring leaf unfolding to warming (S_T). A and **E-J** represent the results of the partial correlation analysis for each plot (**A**), plant functional type (**E**, **F**), biome (**G**, **H**), and climate (**I**, **J**) (the full name of the acronyms in **F**, **H** and **J** can be found in Supplementary Table 4-6). **B**, the coefficients of the global partial correlation. **C**, the importance of each feature based on GINI coefficients and the mean absolute value of SHapley Additive exPlanations (SHAP). **D**, SHAP values based on the global random forest model. *, *P*<0.05; **, *P*<0.01; NS, not significant; P, positive effect; and N, negative effect. The dotted gray lines in **F**, **H**, and **J** mark the transition from significant to non-significant results at *P*<0.05.

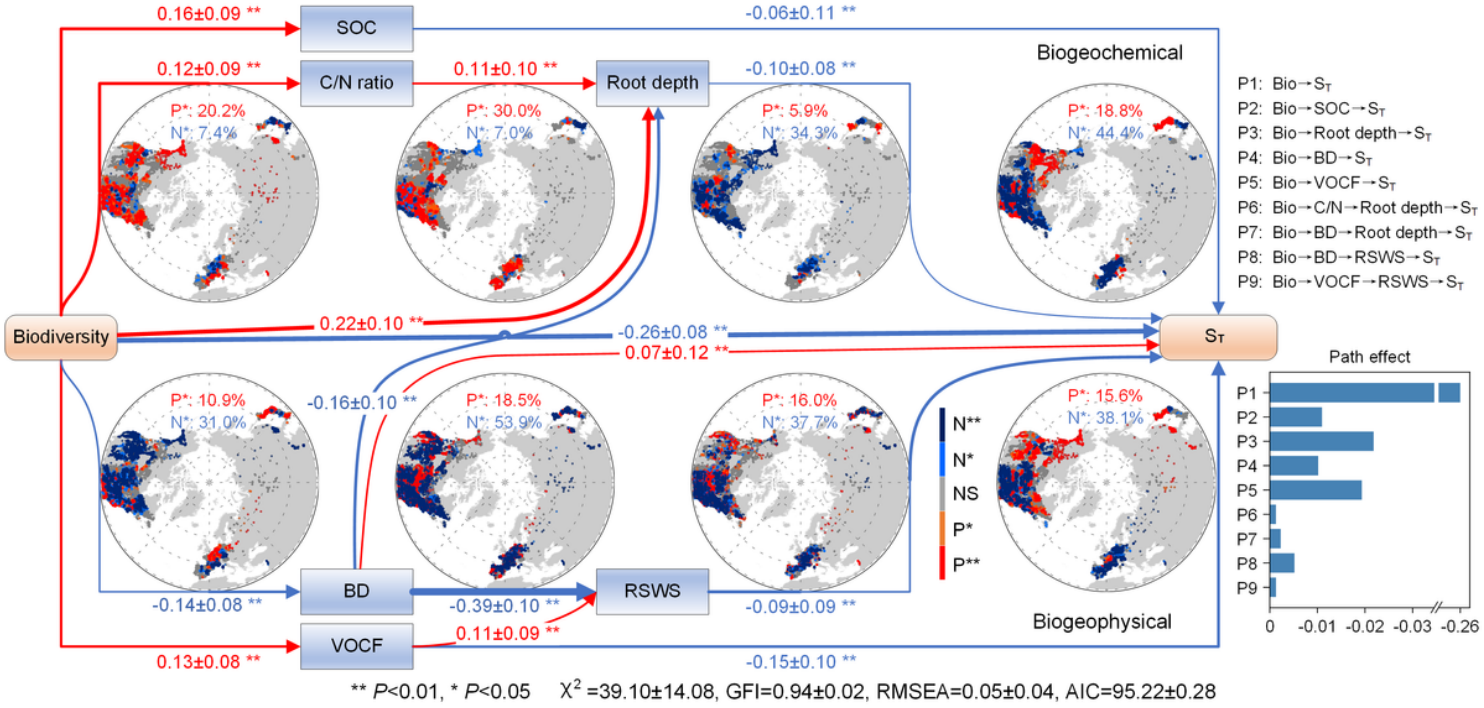

Figure 2

Mechanisms underlying the negative correlation between biodiversity and the sensitivity of spring leaf unfolding to warming (S_T). The figure shows the results of the partial correlation analysis and structural equation modeling (SEM). The coefficients on the path of SEM are standardized, and the circular map on the path represents the spatial distributions of the partial correlation results. The bar chart represents the direct and indirect effects. NS, not significant; P, positive effect; N, negative effect; VOCF, volumetric fraction of coarse fragments; BD, soil bulk density; RSWS, rate of soil warming in spring; SOC, soil organic carbon; and C/N ratio, the ratio of soil concentrations of carbon to total nitrogen.

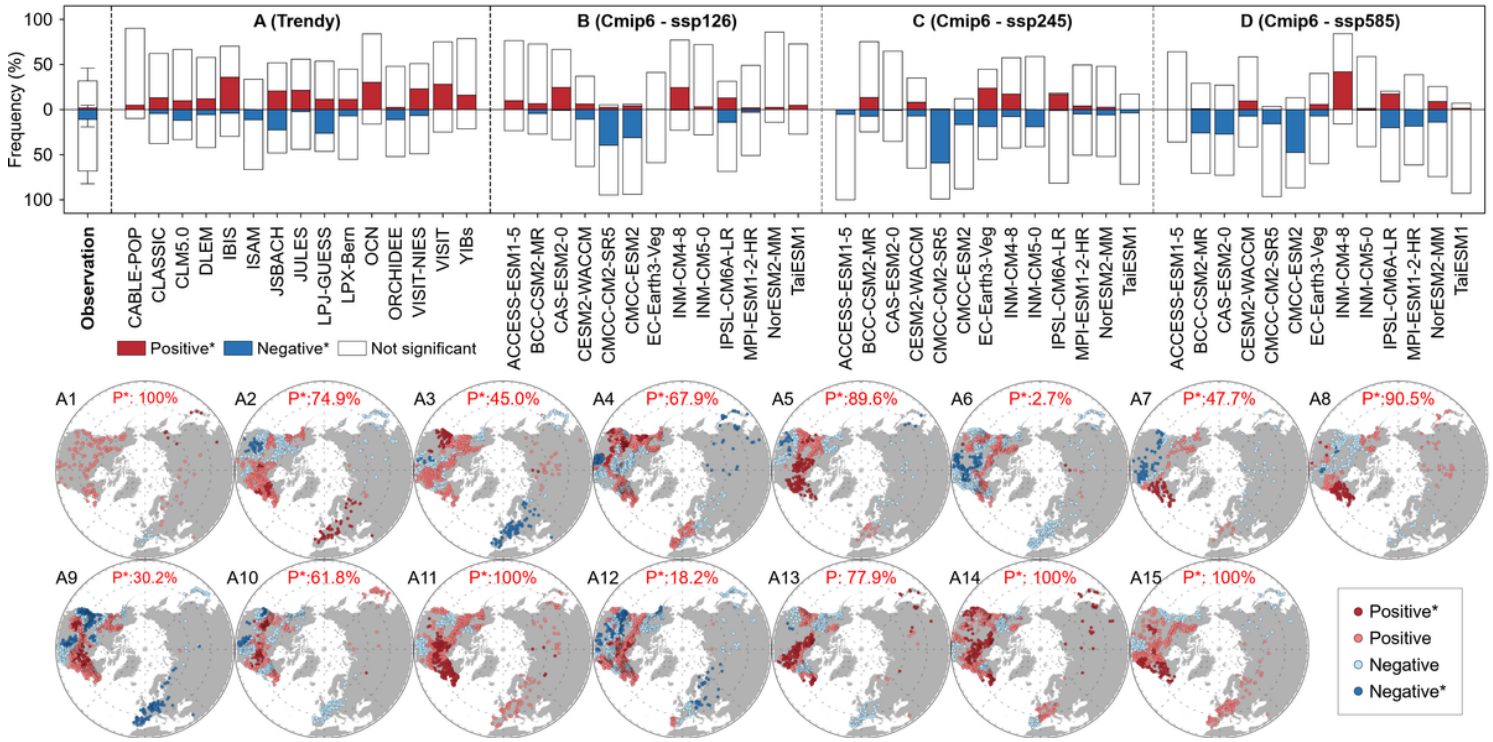

Figure 3

Evaluation of model performances on the sensitivity of spring leaf unfolding to warming (S_T) with biodiversity. A, **B**, **C** and **D** represent results for 15 Trendy models and 13 Earth system models (Cmip6) under different shared socioeconomic pathways (ssp126, ssp245 and ssp585) (See Supplementary Table 2, 3 for model details). **A1**-**A15** represent spatial distributions results for the 15 Trendy models, respectively. The numbers in these figures are percentages of significant positive correlations with respect to all significant correlations. Significance was set at P<0.05.

Supplementary Files

This is a list of supplementary files associated with this preprint. Click to download.

- SupplementalInformation.docx
- ExtendedDataFig.1.png
- ExtendedDataFig.2.png
- ExtendedDataFig.3.png
- ExtendedDataFig.4.png
- ExtendedDataFig.5.png